—研究論文—
Scientific Paper

Paleomagnetic Studies of the Archean Rocks Collected from the Napier Complex in Enderby Land, East Antarctica

Minoru FUNAKI*

東南極，エンダービーランド，ナピアーコンプレックスから採集された始生代岩石の古地磁気学的研究

船木 實*

要旨：南極，エンダービーランド，ナピアーコンプレックスから採集された岩石について古地磁気学的研究を行った．その結果，5個の試料は，交流消磁，熱消磁および磁気履歴特性の測定から，安定な自然残留磁気(NRM)を持つことが判明したが，残りの5個の試料のNRMは不安定であった．安定なNRMは単磁区—擬単磁区構造の磁鉄鉱が担っているが，一部は磁硫鉄鉱が担っている．

最もNRMの方位のばらつきが小さいのは480°Cで熱消磁したときで，その平均のNRMの方位は伏角−82.9°，偏角39.3°，α_{95}=8.2°であった．この値から計算される見かけの磁極(VGP)の位置は，南緯75.0°，東経14.5°である．おそらくこのNRMはナピアーコンプレックスが経験した最後の熱変成 (2.45−2.5b.a.)のときに獲得したと思われる．しかしそのVGPの値は同時期のパイパーのパンゲア，オーストラリア，それにアフリカから求められているVGPの値とは一致しない．このことは，もしNRM獲得年代に問題がなければ，2.5 b.a.には南極，オーストラリアそれにアフリカの大陸はお互いに独立して存在していたと思われる．

Abstract: A total of 10 Archean rocks, collected from the Napier Complex in Enderby Land, Antarctica, were studied paleomagnetically. Natural remanent magnetization (NRM) of 5 specimens is stable supported by AF and thermal demagnetization of NRM, magnetic hysteresis and AF demagnetization of SIRM and ARM properties. The magnetic carriers in the specimens are estimated to be magnetite of single-/pseudosingle-domain structures associated with a small amount of pyrrhotite. However, other 5 specimens have only unstable NRM due to pseudosingle-/multi-domain structures.

The VGP position, 75.0°S latitude and 14.5°E longitude, is calculated from the stable NRM component (−82.9° inclination, 39.3° declination and 8.2° α_{95} value) which is obtained from thermal demagnetization at 480°C. This NRM was acquired at the final metamorphism (2.45−2.5 b.a.) through a cooling stage from 580 to 480°C. The VGP position is very different from apparent polar wander paths around 2.5 b.a. of Piper's Pangaea, Australia and Africa. If the determination of NRM acquisition age is reliable, it suggests the continental rearrangements between the Pangaea of 2.5 b.a. and the early stage of Gondwanaland.

*国立極地研究所. National Institute of Polar Research, 9-10, Kaga 1-chome, Itabashi-ku, Tokyo 173.

1. Introduction

The 23rd Japanese Antarctic Research Expedition (JARE-23) visited Amundsen Bay (68°00′S, 50°30′E) of Enderby Land, East Antarctica, for geoscientific studies in the 1981/1982 austral summer season.

Archean Napier Complex and Proterozoic Rayner Complex comprise the metamorphic rocks of Enderby Land. The terrain around Amundsen Bay belonging to the Napier Complex is estimated to be one of the oldest crusts not only in Antarctica but also in the world (GREW and MANTON, 1979). Therefore, paleomagnetic studies are of interest for the solution of Pangaea problems.

Although a Precambrian paleomagnetic study of Antarctica was reported by EMBLETON and ARRIENS (1973), using the samples of 1 b.a. collected from the Vestfold Hills, there have been no other Precambrian paleomagnetic studies for Antarctica up to present.

The party collected 10 rock samples with orientations for paleomagnetic studies by an engine core drill. As the inclination of the geomagnetic field at the sampling site is about −66.2°, a magnetic compass is available for determination of the sample direction in the field. The sampling site of these samples is shown in Fig. 1. From all core samples, 2 specimens of 1 inch in diameter and length were cut out for measurements of natural remanent magnetizatin (NRM). Collected samples were classified into groups A and B on the basis of grain size and quantity of opaque minerals. The samples of group A are ordinary granulite in this area. It consists essentially of silicate, while opaque grains are not observed with the naked eye. On

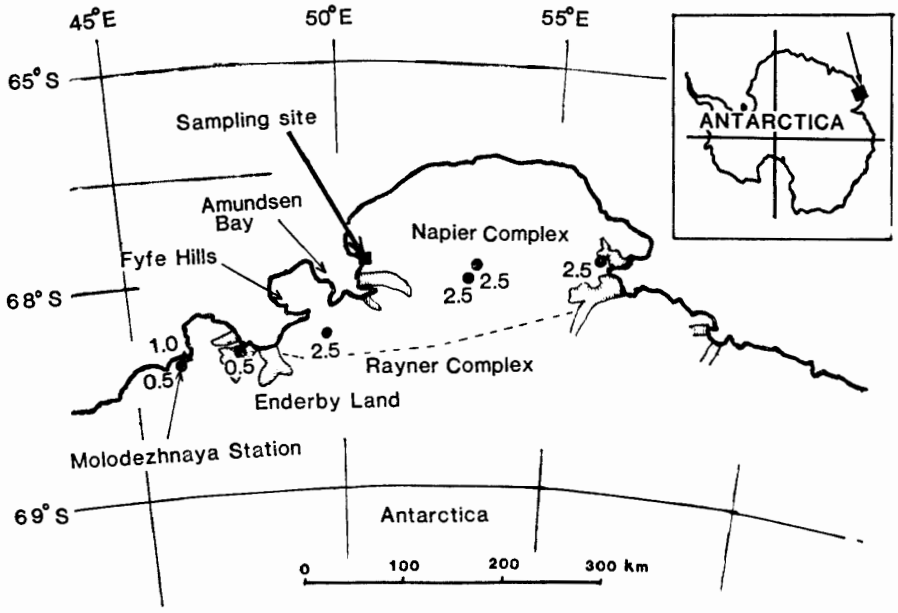

Fig. 1. Sampling site of the Napier Complex in the Amundsen Bay area and geochronologic data (billion years) of the Napier and Rayner Complexs summarized by GREW and MANTON (1979).

the other hand, those of group B consist of a large amount of opaque minerals of 5—10 mm in diameter associated with a minor amount of silicate.

FUNAKI (1984a) reported a preliminary result of NRM for these specimens. Since we have done further paleomagnetic and mineralogical studies, the synthetic results are reported in this paper.

2. Geology and Geochronology

The Napier Complex consists of pyroxene granulite, orthopyroxene-quartz-feldsper gneiss, quartzite and granitiferous gneisses. According to the geological and geochronological studies of this complex (GREW and MANTON, 1979; BLACK and JAMES, 1983; ELLIS, 1983; HARLEY, 1983), an initial acidic ignious crust was formed at 3.7—3.8 b.a. (U-Pb in zircon data supported by Rb-Sr determination age), and then it had three times metamorphisms M1—M3 and deformations D1—D3, and some dyke intrusions. The ages of the respective peak metamorphisms correspond to those of deformation. The inferred ages of metamorphism and dyke intrusion are summarized in Table 1. Metamorphisms M1 (3.1 b.a.) and M2 (2.9 b.a.) are possibly the highest grade regional granulite terrain exposed on the Earth's surface (7—10 k bar, 900—980°C; ELLIS 1980, 1983: SHERATON *et al.*, 1980: GREW, 1981: HARLEY, 1983). The amphibolite·granulite facies M3 metamorphism (2.45—2.5 b.a.) occurred at 650—700°C, 5—8 kbar (HARLEY, 1983). Geochronologic data for Enderby Land summarized by GREW and MANTON (1979) are shown in Fig. 1.

The Rayner Complex was metamorphosed at 1 b.a. under lower P—T conditions than those of the Napier Complex (ELLIS, 1983). The Napier Complex, towards the southwestern margin, had experienced heating, dyke intrusions and shearing possibly related to intense deformation in the amphibolite-granulite facies of the nearby Rayner Complex (BLACK and JAMES, 1983).

Table 1. Metamorphism and chronological data of the Archean rocks from the Napier Complex.

Geological evidence	Age (b.a.)	Method	Remarks
Crustal formation	3.7-3.8	U-Pb, Rb-Sr	Zircon
Metamorphism M1	3.1	Rb-Sr	Granulite
M2	2.9	Rb-Sr	900-950°C 7-10 kbar Amphibolite-granulite
M3	2.45-2.5	Rb-Sr	650-700°C 5-8 kbar
Intrusion	2.35±0.048		Tholeiite dyke
	1.19±0.2		
	0.52		Pegmatite dyke
	0.482±0.003		Alkaline dyke

Accoding to ELLIS (1980, 1983), SHERATON *et al.* (1980), GREW (1981) and HARLEY(1983).

3. AF Demagnetization

Every sample was demagnetized by alternating magnetic field from 0 to 50 mT at intervals of 5 mT. An AF demagnetization curve of a representative specimen in group A is shown in Fig. 2 in Zijderveld diagram. This demagnetization curve can be divided into three parts by the boundaries of 15 and 45 mT. The first part from 0 to 15 mT is a magnetic soft component acquired probably in the present geomagnetic field of sampling site (−66° inclination, −53° declination), because its calculated direction of the soft component is −42° inclination and −34° declination. The second part from 15 to 45 mT is essentially a magnetic hard component, although it shows a small zig-zag decay demagnetization curve. The third part shows breakdown of NRM by 50 mT AF demagnetization. These demagnetization characteristics of group A are essentially similar among the specimens; the original intensities, $6.01-8.79\times10^{-5}$ Am^2/kg, and MDF (median demagnetization field) value about 15 mT are characteristic. Thus, the specimens of group A have magnetic soft and hard components originally, and the hard component is obtained by the minimum AF demagnetization of 15 mT.

The AF demagnetization curve of a specimen belonging to group B is also shown in Fig. 2. It shows very unstable NRM; the horizontal and vertical components decay easily by week demagnetization field of 10 mT. The NRM direction changes widely at the respective demagnetization steps. Original NRM intensities of specimens of this group range from 0.5 to 74.2×10^{-4} Am^2/kg with less than 10 mT MDF value. The NRM intensities are demagnetized more than 70% versus original ones by 15 mT demagnetization. Thus, the specimens in group B have only soft (unstable) NRM.

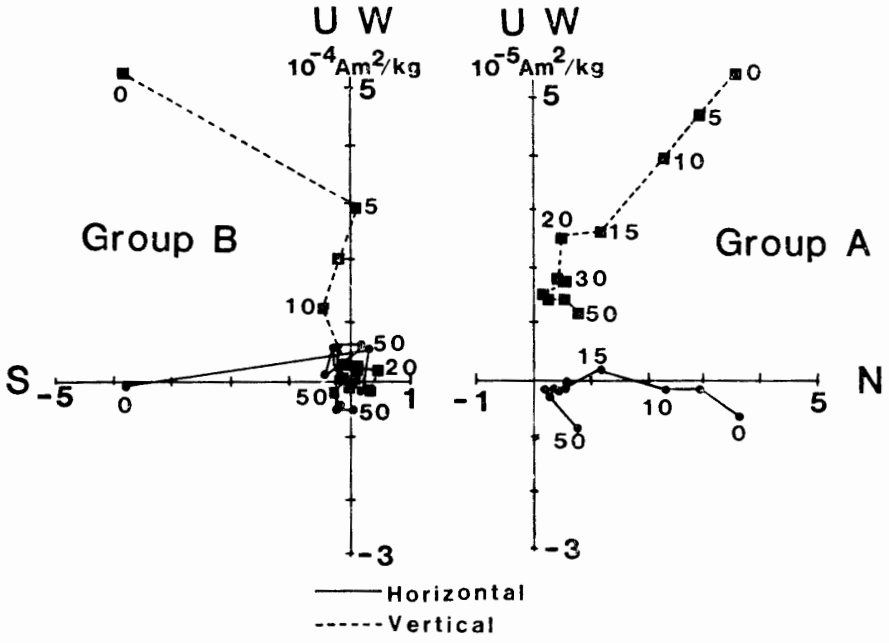

Fig. 2. AF demagnetization curves of NRM by Zijderveld diagram using mT unit of groups A and B specimens.

Table 2. Obtained paleomagnetic results by AF demagnetization of groups A and B specimens from the Amundsen Bay area.

Group	N	Demag (mT)	In ($\times 10^{-5}$Am^2/kg)	Inc	Dec	K	α_{95}	pLat (°S)	pLon (°E)
A	5	0	7.45	−76.5°	302.9°	26	15.0°	-	-
		15	3.76	−84.8	329.4	48	11.1	74.9	71.3
B	5	0	36.79	−80.0	85.2	8	27.4	-	-
		15	10.24	−82.7	279.9	7	29.0	-	-

Demag: AF demagnetization field, In, Inc and Dec: intensity, inclination and declination of mean NRM respectively, K: precision parameter, α_{95}: radius of 95% confidence circle about mean NRM direction, pLat and pLon: paleo-latitude and paleo-longitude of VGP.

The average NRM intensities and the directions before and after AF demagnetization by 15 mT for groups A and B are shown in Table 2, in which, N: sample number, In: mean intensity of NRM, Inc and Dec: mean inclination and declination of NRM, K: precision parameter, α_{95}: radius of 95% confidence, pLat and pLon: paleo-latitude and paleo-longitude of virtual geomagnetic pole (VGP).

The distributions of NRM direction of the group A specimens lead to a good cluster by AF demagnetization to 15 mT: the values of K and α_{95} change from 26 to 48 and from 15.0° to 11.1° respectively. The original mean direction shifts 9.1° in spherical coordinates, with the resultant values Inc = −84.8° and Dec = 329.4°, by this AF demagnetization. The value of In decreases to about 50% from 7.45 to 3.76 $\times 10^{-5}$ Am^2/kg. In the case of the group B specimens, however, the In value decreases to 72% from 36.79 to 10.24$\times 10^{-5}$Am^2/kg. The distributions of original NRM direction do not change to make a cluster by that AF demagnetization. Consequently, the VGP position is obtained from the group A specimens as pLat = 74. 9° S and pLon = 71.3° E by the AF demagnetization, as shown in Table 2.

4. Thermal Demagnetization

The thermal demagnetization test has been applied in air to all specimens of group A from 30 to 580°C at intervals of 50° C. The typical demagnetization curves of two specimens (a) and (b) are shown in Fig. 3, where (a) is thermal demagnetization curves of original NRM and (b) is that after AF demagnetization to 15 mT. The intensity demagnetization curves of the two cases are essentially similar from 130 to 580°C, although they are very different from 30 to 130°C. This difference is due to the existence of the magnetic soft component in specimen (a) and to its absence (already demagnetized) in specimen (b). In the directional change curves, the direction change resulting in the soft magnetic component is observed from 30 to 130°C in specimen (a). In the range from 130 to 480°C, the relatively smooth demagnetization area may be divided into two parts at 330°C; the one decreases but the other increases gradually. The NRM directions of the specimens of group A change systematically in the same direction as that makes a cluster by the thermal demagnetization in this range. From 480 to 580°C, the magnetizations decay steeply, and finally small magnetiza-

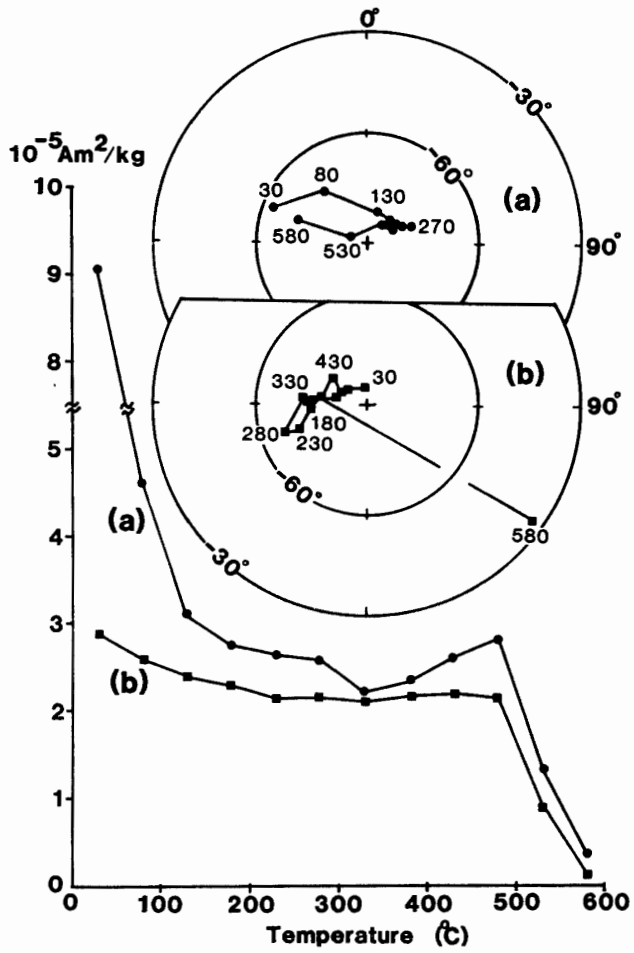

Fig. 3. Thermal demagnetization curves for group A specimens. (a): original specimens (a), (b): specimen (b) which was AF demagnetized up to 15 mT.

tions less than 5% versus original one are observed. As the directions between 480 and 580°C are scattered widely from the clusters, there are no significant magnetizations in these specimens at such temperatures.

5. Basic Magnetic Properties

Basic magnetic properties, thermomagnetic curves, magnetic hysteresis properties and acquisition and demagnetization of SIRM (saturation isothermal remanent magnetization) and ARM (anhysteresis remanent magnetization) were measured in order to establish the reliability of NRM of the representative specimens from groups A and B.

Thermomagnetic curves were obtained with a vibrating sample magnetometer, at 1.1×10^{-2} Pa pressure, with an applied magnetic field intensity of 1 T and heating and cooling rate of 200°C/h. The saturation magnetizations before heating at 1 T are 0.43 Am^2/kg for the specimens of group A and 4.83 Am^2/kg for those of group B.

The thermomagnetic curves of the 1st run from the group A specimens (Fig. 4) are irreversible, presenting a clearly defined Curie point of magnetite at 580°C and a

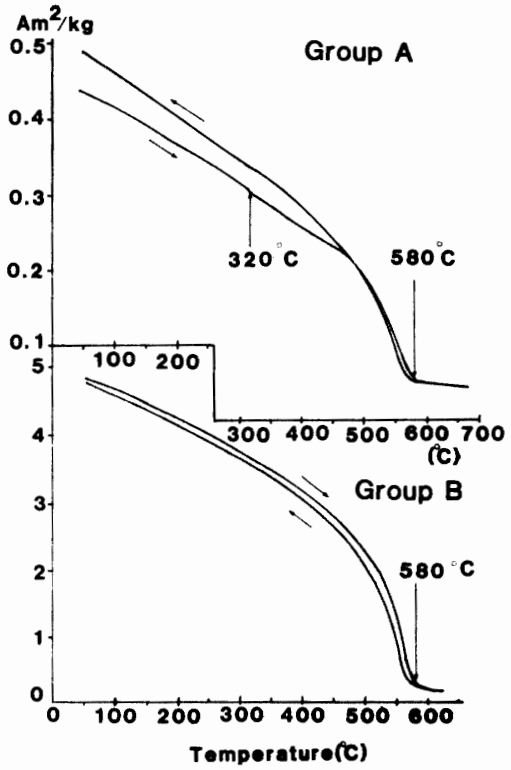

Fig. 4. Thermomagnetic curves obtained by 1 T for groups A and B specimens.

minor Curie point at 320°C and a small gradual natural change around 400°C in the heating curve and 580°C in the cooling curve. The intensity of saturation magnetization after the 1st run heating increased by about 13% at room temperature. The 2nd run thermomagnetic curves of this specimen are consistent with the 1st run cooling curves. The Curie point 580°C is clearly ascribed to magnetite. The Curie point at 320°C, observed only in the 1st run heating curve, is consistent with the phase transition temperature of pyrrhotite. A natural change magnetization around 400°C in the 1st run heating curve may be due to the chemical alteration from maghemite or iron sulfide to magnetite, because it was not observed in the cooling curve and in the 2nd run cycle.

On the other hand, the thermomagnetic curves of the group B specimens (Fig. 4) are reversible with the clearly defined Curie point at 580°C. It suggests that the magnetic mineral in group B specimens is defined only as pure magnetite.

The basic magnetic hysteresis curves were measured with a vibrating sample magnetometer at room temperature. The saturation magnetization (I_S), the saturation remanent magnetization (I_R), the coercive force (H_C) and the remanent coercive force

Table 3. Magnetic hysteresis properties of groups A and B specimens.

Group	I_S Am^2/kg	I_R Am^2/kg	H_C mT	H_{RC} mT	I_R/I_S	H_{RC}/H_C
A	0.31	0.048	11.3	33.2	0.16	2.9
B	4.53	0.245	5.5	19.4	0.05	3.5

(H_{RC}) are determined from these curves. The values for groups A and B specimens are listed in Table 3. The values of I_S indicate the amount of ferrimagnetic or ferromagnetic minerals in the specimens. According to the thermomagnetic analysis, the magnetization of groups A and B specimens are essentially due to magnetite in the original specimen. Since the saturation magnetization of magnetite (I_S (M_t)) is 92 Am^2/kg in 24°C, its content in groups A and B specimens (V_A, V_B) is calculated as $V=I_S/I_S$ (M_t). If the magnetization, resulting in the minor Curie point at 320°C, is neglected for group A specimens, the amount of magnetite for groups A and B specimens was found to be 0.34 and 4.92 wt%, respectively.

DAY *et al.* (1977) investigated the relationships between domain structures and grain size, using the magnetic hysteresis properties of the I_R/I_S and H_{RC}/H_C. Their results showed that the experimental critical size of single-domain behavior for magnetite grains was about 0.1 μm; multi-domain grains were characterized by $H_C <$ 5mT, $H_{RC}/H_C > 4$ and $I_R/I_S < 10^{-2}$, having no compositional dependence for more than 150 μm in diameter of magnetite and titanomagnetite. As shown in Table 3, the values of I_R/I_S and H_{RC}/H_C are 0.16 and 2.9 for group A and 0.05 and 3.5 for group B specimens, respectively. It suggests, therefore, that the domain structures are single-/pseudosingle-domains for the group A specimens and pseudosingle-/multi-domains for the group B specimens.

From the representative specimens of groups A and B the SIRM and ARM were acquired in order to test the stability against AF demagnetization. The steady magnetic field for SIRM acquisition is 1.5 T. The direction of a steady biasing-magnetic field ($\bar{h}$) is parallel to the $+z$ axis of the specimens and alternating magnetic field ($\tilde{H}$) for ARM acquisition tests. These magnetic field intensities are given as $\bar{h}=$ 0.044 mT and $\tilde{H}=130$ mT. The obtained AF demagnetization curves of their remanence are shown in Fig. 5. JOHNSON *et al.* (1975) examined the stability of ARM and SIRM against AF demagnetization for fine-grained and coarse-grained magnetite

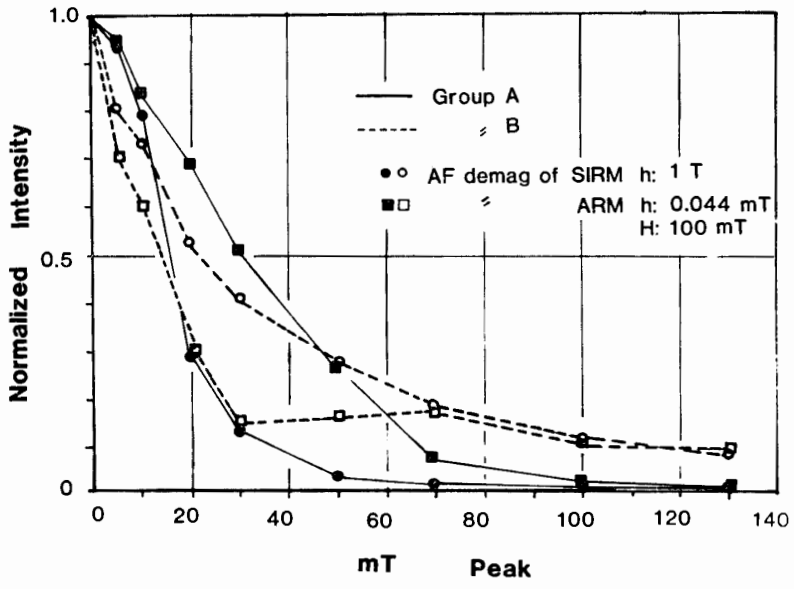

Fig. 5. AF demagnetization curves of SIRM and ARM for groups A and B specimens.

particles. According to their results, the stability of ARM is higher than that of SIRM in single-domain (fine-grained: 0.2 μm) particles and *vice versa* in multi-domain (coarse-grained: 210−250 μm) ones. Their method did not show the difference between single-/multi-domain and pseudosingle-domain structures. However, there is a possibility that the single-/pseudosingle-domain boundary lies around 0.2 μm grain size at least. These stability sequences of our specimens are in the order ARM> SIRM for the group A specimens, and SIRM>ARM for the group B ones. Namely, this suggests that the magnetite grain structure is single-domain for the group A specimens and is multi-domain for the group B specimens.

6. Mineralogy

The representative specimens from each group were polished for reflected light microscopical observations and electron prove microscopic analyses (EPMA). In the group A specimens, magnetite, ilmenite and iron sulfide grains were observed as opaque minerals. The magnetite grains, being 250 μm in maximum diameter, were cut by the fine lath of ilmenite lamellae. These exsolution textures are observed only in magnetite grains larger than 100 μm in diameter. However, the number of such large grains is very small, only several grains in the surface of about 6 cm^2 in area. Countless small magnetite grains, less than 20 μm in diameter, are present along the boundary of silicate grains. On the surface of these magnetite grains, maghemite structures are not observed by 1000 times magnification microscope. Very small iron sulfide grains (less than 20 μm) are also scattered along the boundary of silicate grains but the abundance is smaller than that of magnetite grains. The representative chemical compositions of opaque minerals in the group A and B specimens were analyzed with EPMA listed in Table 4. The analysis indicates that magnetite (Fe_3O_4), ilmenite ($FeTiO_3$), pyrite (FeS_2) and pyrrhotite (Fe_7S_8-FeS) are included in the group A specimens. It also suggests that the magnetite grains are almost pure associated with small amounts of SiO_2, Al_2O_3, TiO_2 and Cr_2O_3 for the both groups specimens.

In the group B specimens, the opaque minerals are identified as magnetite, iron sulfide and hercynite ($FeAl_2O_4$) by optical observations and EPMA analyses as listed in Table 4. The large magnetite grains more than 15 mm in length, extending into the silicate matrix, have well-developed exsolution lamellae of the hercynite and the ilmenite, although these lamellae dominate in hercynite rather than in ilmenite laths. On the other hand, the small magnetite grains less than 30 μm in diameter, having no lamella or maghemite texture, are also observed in the silicate grains. Small pyrite grains less than 20 μm were observed along the silicate grains. Therefore, magnetic minerals of the group B specimens are almost pure magnetite.

7. Discussions

Clearly defined magnetic minerals in the group A specimens are almost pure magnetite which is a main magnetic mineral in these specimens as supported with thermomagnetic and EPMA analyses. The minor Curie point at 320°C, observed in

Table 4. Chemical analyses of opaque grains in groups A and B specimens by EPMA.

Oxide minerals

	Magnetite					Ilmenite						Hercynite	
	Group A		Group B			Group A			Group B			Group B	
SiO_2	0.078	0.316	0.199	0.151	0.133	0.033	0.940	0	0.120	0.092	0.127	0.253	0.092
Al_2O_3	0.217	0.380	0.733	0.270	0.298	0.029	0.203	0.030	3.497	0.950	0.008	56.481	56.783
TiO_2	0.340	0.095	0.131	0.104	0.071	50.389	48.015	51.268	49.649	50.045	51.656	0.053	0.033
Cr_2O_3	0.212	1.978	0.155	0.045	0.109	0.153	0.084	0.207	0	0.023	0.031	0.210	0.218
NiO	0.069	0	0.089	0	0.064	0	0.066	0.112	0.097	0	0.010	0.110	0
MgO	0.017	0.101	0.024	0.021	0.024	0.643	1.103	0.881	0.422	0.201	0.255	3.856	4.355
FeO	89.348	86.349	89.668	89.861	91.620	47.334	47.515	47.184	44.805	48.370	47.386	35.784	36.496
MnO	0	0	0.038	0.048	0.038	0.348	0.634	0.447	0.402	0.161	0.270	0.033	0.077
CaO	0.020	0.049	0.012	0	0	0.042	0.266	0	0.023	0.015	0.010	0.016	0.022
Na_2O	0.037	0	0.074	0.062	0	0	0.057	0.018	0	0	0.004	0.027	0.094
K_2o	0.012	0.047	0.006	0	0.036	0	0.062	0	0	0	0	0	0.009
Total	90.349	89.315	91.130	90.562	92.393	98.971	98.944	100.147	99.015	99.858	99.756	96.823	98.154

Sulfide minerals

	Pyrrhotite			Pyrite				
	Group A			Group A			Group B	
Fe	60.5116	60.4749	58.9031	44.0086	47.7140	46.9548	46.3669	45.8223
Ni	1.6730	1.7744	1.6720	0.0124	0.2597	1.6431	0	0.0906
Co	0.0525	0.1332	0.0122	3.2671	0.7912	0.1543	2.1011	2.6566
S	40.0252	38.6846	39.2252	53.1460	53.4708	52.9247	53.9391	54.2359
Total	102.2623	100.9971	99.8125	100.4341	102.2356	101.6769	102.4071	102.8054

the 1st run heating thermomagnetic curve, is consistent with the phase transition temperature from the monocrinic pyrrhotite of the ferrimagnetism to the hexagonal one or troilite (hexagonal) of the paramagnetism. It is possible that this temperature is due to titanomaghemite Curie point 320°C, but it cannot be adopted by the results of EPMA analyses and microscopic observations.

The specimens of group A have both soft and hard magnetic components, as confirmed by AF and thermal demagnetization tests. The hard one can be obtained by AF demagnetization to 15 mT or thermal demagnetization to 130°C. The NRM-resultant pyrrhotite cannot usually be reliable paleomagnetically due to its magnetic anisotropy and mineral-forming age. Therefore, reliable NRM seems to be obtained only by thermal demagnetization from higher temperature than pyrrhotite Curie point 320°C to lower than magnetite one 580°C (from 330 to 530°C in this case). Significant NRM directions are obtained by thermal demagnetization from 330 to 480°C, because of the NRM stability for the specimens of group A. Since the NRM intensities decay steeply from 480 to 580°C, the reliable NRMs would have been acquired when the Napier Complex came through such a temperature range during the final cooling stage.

The magnetite grains in the group A specimens are estimated to be substantially single-/pseudosingle-domain structures by the evidence of magnetic hysteresis properties, SIRM and ARM tests and AF demagnetization tests. However, such magnetite grain sizes considerably exceed the critical size of the single-/pseudosingle-domain structure (less than 2 μm; JOHNSON *et al.*, 1975). The possible explanation is that these magnetite grains are cut by fine ilmenite laths not only in the case of large grains as observed by microscope but also in the case of small grains. Probably, the fine laths in small grains can not be observed due to the smaller scale below the discrimination capacity of the optical microscope.

Magnetic minerals in the group B specimens are defined only as almost pure magnetite grains from the evidence of the Curie point 580°C and EPMA analyses. These specimens have only soft magnetic component from the results of AF

Table 5. Change of average NRM against thermal demagnetization of 5 specimens from group A.

Temperature (°C)	In Am²/kg	Inc	Dec	K	α_{95}	pLat (°S)	pLon (°E)
30	6.50	−78.3°	201.5°	4	43.5°	45.4	62.5
80	2.98	−85.0	289.3	12	22.1	68.2	77.0
130	3.13	−77.0	322.5	21	16.8	75.3	125.7
180	2.65	−82.3	340.2	32	13.5	79.9	81.3
230	2.37	−84.4	339.5	28	14.5	76.8	68.2
280	2.26	−85.0	316.0	27	14.8	72.7	74.8
330	2.06	−85.4	331.1	33	13.3	74.3	67.5
380	2.23	−85.9	5.6	55	10.3	75.0	47.9
430	2.28	−85.8	41.6	63	9.6	72.4	32.5
480	2.32	−82.9	39.3	86	8.2	75.0	14.5
530	1.19	−83.1	314.6	54	10.4	73.5	87.3
580	0.36	13.3	196.5	-	-	-	-

The notations are consistent with Table 2.

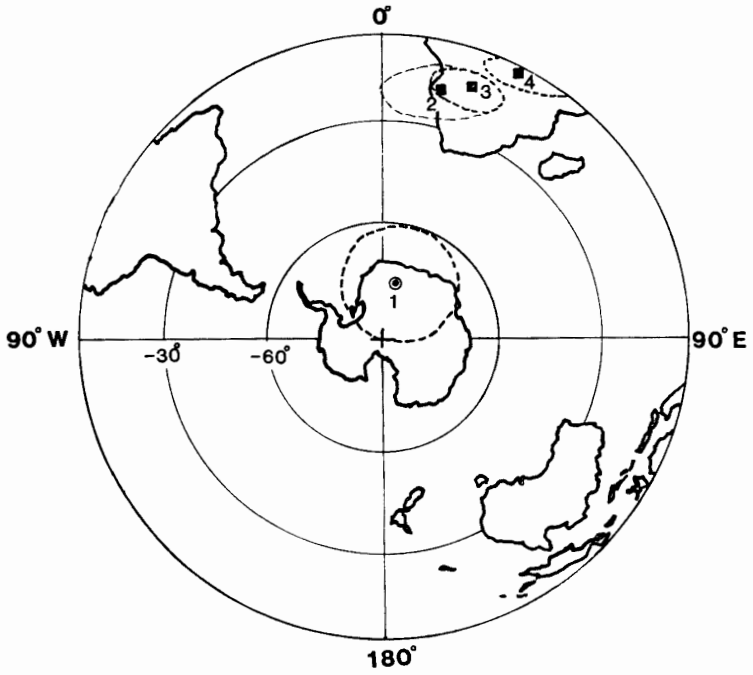

Fig. 6. VGP positions from 2.5 b.a. to Cambro—Ordovician age for Antarctica. (1): 2.5 b.a. (this study), (2): 1.0 b.a. (EMBLETON and ARRIENS, 1973) and (3, 4): Cambro—Ordovician age (FUNAKI, 1984 b; MCQUEEN et al., 1972).

demagnetization analysis. This is caused by pseudosingle-/multi-domain structures of magnetite grains. It is supported by the magnetic hysteresis properties and the ARM and the SIRM tests. Although these grains were cut by the hercynite and ilmenite laths, the magnetic domains are still multi-domain structures. It is concluded for the specimens of group B that observed NRMs originate both of IRM and VRM related to the present geomagnetic field.

The mean NRM changes of 5 specimens from group A by thermal demagnetization are listed in Table 5. As mentioned above, reliable NRM is obtained only by thermal demagnetization from 330 to 480°C. The declination of mean NRM changes systematically from 331.1 to 39.3° for the respective temperature from 330 to 480°C, while its inclination shows almost no shift. However, the angular deviation of NRM between 330 and 480°C is 13.6°, but they cannot be fully separated taking their α_{95} values into consideration. Since the best clustering $\alpha_{95}=8.2°$ and K=86 is observed at 480°C of thermal demagnetization, significant mean NRM is obtained by that demagnetization temperature. Therefore, the VGP positions are derived as Inc= −82.9°, Dec=39.3° and paleo-latitude pLat=75.0°S, paleo-longitude pLon=14.5°E at thermal demagnetization 480°C for the Amundsen Bay area as shown in Fig. 6 (number 1).

As mentioned above, the Napier Complex had experienced two times of granulite (M1 and M2) and one time of amphibolite (M3) facies metamorphisms, and then four times of dyke intrusions (BLACK and JAMES, 1983). Since the estimated maximum temperature of final metamorphism M3 would be 650—700°C, it exceeds the magnetic Curie point 580°C of the group A specimens. As a consequence, the acquired magnetizations at M1 and M2 metamorphisms must have disappeared and

the complex was remagnetized to the geomagnetic field direction at that time. On the other hand, the thermal influence resulting from dyke intrusions after M3 metamorphism could be neglected by the following estimation. According to CARSLAW and JAEGER (1959), if a completely molten dyke at 1100°C intruded into a granite body, the maximum temperature of the granite does not exceed 200°C at a point of a distance of the dyke thickness from its surface. There is no evidence of dyke intrusions around the sampling site. Therefore, the granulite of the Napier Complex recorded the geomagnetic field when the Complex was finally metamorphosed by M3 metamorphism at 2.45−2.5 b.a. ago.

EMBLETON and ARRIENS (1973) reported a VGP position of the Archean age (1.0 b.a.) from the Vestfold Hills near Davis Station of Australia (68°35′S, 77°58′E) in East Antarctica. They obtained the mean direction of NRM as Dec=−42.5°, Inc=107.5° with $\alpha_{95}=11°$. The calculated VGP position from this NRM direction is pLat=17°S, pLon=13°E, as shown in Fig. 6 (number 2). This position is very close to the Cambro−Ordovician (about 0.5 b.a.) VGPs obtained from East Antarctica (Fig. 6, numbers 3 and 4) reported from the McMurdo Sound (FUNAKI, 1984b) and Mirny Station (MCQUEEN *et al.*, 1972) respectively. It can be understood that the VGP position of 2.5 b.a. obtained from the Napier Complex is completely different from the VGP of the Cambro−Ordovician and the Proterozoic ages.

There are two ideas about apparent polar wander (APW) paths of Precambrian age. The first one proposed by PIPER (1982) is that most of the continental crust was once grouped into a single vast continent (Piper's Pangaea); all the paleomagnetic poles from the major shields conform to a single narrow path for the whole from 2.6 to 0.57 b.a. The second one is an idea critical of Piper's Pangaea, as proposed by *e.g.* IRVING and MCGLYNN (1979); there is no paleomagnetic evidence for the proposition that the continental crust was assembled into a single unchanged Pangaea during

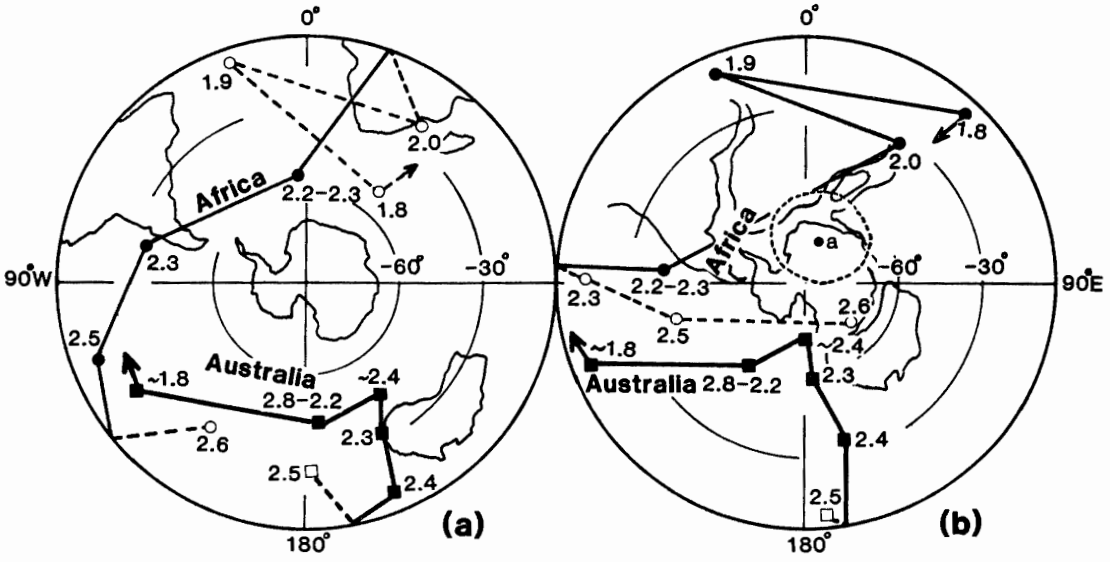

Fig. 7. APW Paths from 2.5 to 1.8 b.a. for Australia and Africa and the VGP position of 2.5 b.a. obtained by this study. (a): original APW paths, (b): after rotation of the APW path referred to the Gondwana reconstruction model presented by SMITH and HALLAM (1970).

the whole interval of 2.2−1.3 b.a. The VGP position of the Napier Complex is compared with the APW paths of 2.45−2.5 b.a. from Piper's Pangaea, Australia and Africa. Although the APW path of Piper's Pangaea comes through a region of relatively low latitudes (PIPER, 1982), that of the Napier Complex, showing high latitudes, does not overlap taking α_{95} value into consideration. The VGP positions from the Archean to the Proterozoic ages were listed by MCELHINNY (1973) for Africa and by EMBLETON (1981) for Australia. The APW paths in Fig. 7a are drawn based on these VGP positions. When the paths are rotated to Antarctica referred to the Gondwana reconstruction model presented by SMITH and HALLAM (1970), they are shifted as shown in Fig. 7b. It shows that the latitude, the longitude and the angle of their rotation are 1.3°N, 36°W and −58.4° for Africa, and −3.6°S, 40°E and −31° for Australia, respectively. These APW paths after rotation do not overlap each other, and furthermore the obtained VGP position from the Napier Complex does not overlie these APW paths around 2.5 b.a. taking the α_{95} value into consideration as shown in Fig. 7b. However, the paleomagnetic results obtained from the southern continents including India support the presence of Gondwanaland from the early Paleozoic to the Jurassis period (*i.e.* CREER, 1970; MCELHINNY, 1973). From these viewpoints, it is necessary to explain some continental rearrangements between the Pangaea of 2.5 b.a and the early Gondwanaland.

8. Conclusion

Natural remanent magnetization of the Napier Complex at Amundsen Bay is superposition of magnetic hard and soft components, although the samples having large opaque grains have only the soft one. The soft NRM is demagnetized completely by AF demagnetization to 15 mT and by thermal demagnetization to 130°C. The hard NRM is originated from the resultant magnetite and pyrrhotite. Fine-grained magnetite carries reliable NRM which was magnetized mainly through 580 to 480°C in the cooling stage of the final metamorphism M3 at 2.5 b.a. ago. The reason to have reliable NRM for magnetite is due to single-/psuedosingle-domain structure, supported by magnetic hysteresis data, AF demagnetization, ARM and SIRM tests and microscopic observations.

The most reliable VGP position at 2.5 b.a. ago is 75.0°S in latitude and 14.5°E in longitude which is obtained from stable NRM direction (−82.9° inclination, 39.3° declination) by thermal demagnetization to 480°C. This position is very different from the VGP positions reported from rocks of Proterozoic and lower Paleozoic ages in East Antarctica. The VGP position obtained from the Napier Complex is very different from the APW paths for 2.5 b.a. of Piper's Pangaea, Australia and Africa, suggesting that the continental rearrangements between the Pangaea of 2.5 b.a. and the early Gondwanaland may be necessary, if dating of the rocks is reliable.

Acknowledgments

The author wishes to thank Prof. T. HOSHIAI (National Institute of Polar Research, NIPR), and Prof. Y. YOSHIDA (NIPR) for their paleomagnetic and

geological suggestions and encouragements.

Thanks are also due to Drs. D. MATSUEDA and Y. MOTOYOSHI for supplying the samples and for their useful discussions and due to Mr. H. KOJIMA for his EPMA measurements.

References

BLACK, L. P. and JAMES, P. R. (1983): Geological history of the Archaean Napier Complex of Enderby Land. Antarctic Earth Science, ed by R. L. OLIVER *et al.* Canberra, Aust. Acad. Sci., 11–15.

CARSLAW, H. S. and JAEGER, J. C. (1959): Conduction of Heat in Solid. 2nd. ed. Oxford, Oxford Univ. Press, 54.

CREER, K. M. (1970): A review of palaeomagnetism. Earth-Sci. Rev., **6**, 369–466.

DAY, R., FULLER, M. and SCHMIDT, V. A. (1977): Hysteresis properties of titanomagnetites: Grain-size and compositional dependence. Phys. Earth Planet. Inter., **13**, 260–267

ELLIS, D. J. (1980): Osumilite-sapphirine-quartz granulites from Enderby Land, Antarctica: P–T conditions of metamorphism, implications for garnet-cordierite equilibria and the evolution of the deep crust. Contrib. Mineral. Petrol., **74**, 201–210.

ELLIS, D. J. (1983): The Napier and Rayner complexs of Enderby Land, Antarctica–Contrasting styles of metamorphism and tectonism. Antarctic Earth Science, ed. by R. L. OLIVER *et al.* Canberra, Aust. Acad. Sci., 20–24.

EMBLETON, B. J. J. (1981): A review of paleomagnetism of Australia and Antarctica. Paleoreconstruction of the Continents. Washington, D. C., Am. Geophys. Union, 78–79 (Geodyn. Ser., **2**).

EMBLETON, B. J. J. and ARRIENS, P. A. (1973): A pilot study of the paleomagnetism of some Pre-Cambrian dykes from East Antarctica. Geophys. J. R. Astron. Soc., **33**, 239–245.

FUNAKI, M. (1984a): Natural remanent magnetization of the Napier Complex in Enderby Land, East Antarctica. Nankyoku Shiryô (Antarct. Rec.), **83**, 1–10.

FUNAKI, M. (1984b): Investigation of the paleomagnetism of the basement complex of Wright Valley, Southern Victoria Land, Antarctica. J. Geomagn. Geoelectr., **36**, 529–563.

GIDDINGS, J. W. (1976): Precambrian paleomagnetism in Australia I: Basic dykes and volcanics from the Yilgarn Block. Tectonophysics, **30**, 91–108.

GREW, E. S. (1981): Granulite-facies metamorphism at Molodezhnaya Station, East Antarctica. J. Petrol., **22**, 297–336.

GREW, E. S. and MANTON, W. I. (1979): Archean rocks in Antarctica: 2.5 billion-year uranium-lead ages of pegmatites in Enderby Land. Science, **206**, 443–444.

HARLEY, S. L. (1983): Regional geobarometry-geothermometry and metamorphic evolution of Enderby Land, Antarctica. Antarctic Earth Science, ed. by R. L. OLIVER *et al.* Canberra, Aust. Acad. Sci., 25–30.

IRVING, E. and MCGLYNN, J. C. (1979): Palaeomagnetism in the Coronation Geosyncline and arrangement of continents in the middle Proterozoic. Geophys. J. R. Astron. Soc., **58**, 309–336.

JOHNSON, H. P., LOWRIE, W. and KENT, D. V. (1975): Stability of anhysteretic remanent magnetization in fine and coarse magnetite and maghemite particles. Geophys. J. R. Astron. Soc., **41**, 1–10.

MCELHINNY, M. W. (1973): Paleomagnetism and plate tectonics. Cambridge, Cambridge Univ. Press, 233p.

MCQUEEN, K. M., SCHARNBERGER, C. K., SCHARON, L. and HALPERN, M. (1972): Cambro-Ordovician paleomagnetic pole position and rubidium-strontium total rock isochron for charnockitic rocks from Mirny Station, East Antarctica. Earth Planet. Sci. Lett., **16**, 433–438.

PIPER, J. D. A. (1982): The Precambrian palaeomagnetic record; The case for the Proterozoic supercontinent. Earth Planet. Sci. Lett., **59**, 61–89.

SHERATON, J. W., OFFE, L. O., TINGEY, R. J. and ELLIS, D. J. (1980): Enderby Land, Antarctica—An unusual Precambrian high grade metamorphic terrain. Geol. Soc. Aust., **27**, 305—317.
SMITH, A. G. and HALLAM, A. (1970): The fit of the southern continents. Nature, **225**, 139—144.

(Received November 13, 1987; Revised manuscript received December 17, 1987)